EXPERIMENTAL INVESTIGATION OF HEAT TRANSFER OF FLOWING LIQUID FILM WITH INSERTED METAL FOAM LAYER SUBJECTED TO AIR JET IMPINGEMENT

by

Yunsong ZHANG, Wei CHEN*, Wei LI, and Xiao ZHU

Merchant Marine College, Shanghai Maritime University, Shanghai, China

Original scientific paper
https://doi.org/10.2298/TSCI171014080Z

In this paper, coupling the air jet impingement and the copper metal foam above flowing liquid film were employed to enhance the heat transfer. The thickness of flowing liquid film can be controlled owing to the application of the metal foam above the film, and its solid matrix extends the air-liquid-solid interface of heating surface. The evaporated water can be supplied by the capillary force in the porous layer. The experiments were conducted to investigate the performances of the flowing liquid film with inserted porous layer subjected to impinging jet air. The air jet velocity, the flow rate and thicknesses of the liquid film as well as the porosity of metal foam influence the surface temperature of heated wall and the corresponding local heat transfer coefficient greatly. The change ratios of heat transfer coefficient due to the above factors were presented. More cooling can be obtained on the heated wall in the flowing liquid film with inserted porous layer subjected to impinging jet air while the higher liquid film velocity and air jet velocity, the thinner liquid film and the lower porosity of metal foam occur.

Key words: *liquid film, porous medium, air jet impingement, heat transfer*

Introduction

The heat and mass transfer characteristics of thin liquid films have been widely utilized in various engineering fields, such as electronic components cooling, microprocessors, and heat dissipation of power machinery [1-3]. The decline in thermal resistance and the increase in vapor transport across the liquid-vapor interface can significantly improve the liquid film heat transfer [4]. The minimizing of liquid film thickness for lower thermal resistance is vital for the heat transfer, but the risk of dryout is also brought. With the addition of porous medium, the capillary force supplied by the porous medium can drive the liquid film to maintain controllable thickness, thus the occurrence of dryout could be effectively avoided [5]. Also the application of pump-assisted force can provide extra power that exceeds the original capillary limit [6]. Meanwhile, the convective disturbance and phase change could be all strengthened by the particular spatial structure and the larger surface area of porous material [7].

Covering porous medium above the heated surface is often employed to improve the heat transfer of flowing liquid film. The material property, capillary effect, and the flowing mode have a profound influence on the liquid film heat transfer in porous structures. Sosnowski *et al*. [8] analyzed the effect of material physical properties, film inner buoyancy and temperature difference on liquid film evaporation. The liquid film thickness, liquid film flowing rate,

* Corresponding author, e-mail: weichen@shmtu.edu.cn

porous medium property and the temperature difference can considerably impact the heat and mass transfer of both falling and horizontal liquid film evaporation [9-12]. Narayanan *et al*. [13, 14] experimentally and numerically analyzed the manufactured cooling system of thin liquid film covered by porous membrane subjected to jet air and showed that with the heat flux of 500 W/cm^2, the surface temperature of hot wall reached nearly 360 K under saturation temperature of liquid.

The introduction of air jet impingement on liquid film heat transfer fruitfully promotes the mixture and diffusion effect of vapor and air, as well as decreases the saturation extent of generated vapor to enhance the phase change progress. Zhao [15] studied the influencing factors including the Peclet number, the Lewis number, the temperature, and the relative humidity of air, and illustrated that all these factors could have great impact on the heat transfer of heated porous bed at stagnation point. Wong and Indran [16], Wong and Saeid [17, 18], and Wong [19] studied the air jet impinging on metal foam heat sink and plate heat sink, respectively. The research showed that the heat transfer efficiency of the former is greater than that of the latter, and the low-porosity metal tended to perform better than that of high-porosity one on the total heat transfer. Dorea and De Lomos [20] and Yakkatelli [21] analyzed the turbulent and laminar jet impinging, respectively and showed the effect of permeability and porosity of porous material on jet flowing state.

Previous studies have demonstrated that both the porous medium and air jet impingement can effectively promote the heat transfer of flowing liquid film. However, few experimental researches have focused on the coupling of porous metal foam and air jet impingement on the heat transfer of liquid film, and the internal mechanism of those influencing factors and the interaction affecting the heat transfer performance of flowing liquid film need to be investigated further. In this paper, the heat transfer performance of flowing liquid film with inserted porous layer subjected to air jet impinging was experimentally investigated. The flowing liquid film heat transfer was experimentally conducted at various liquid film velocities, air jet velocities, liquid film thicknesses and porous layer porosities, respectively. The collected results of heated wall temperature and corresponding local heat transfer coefficient were compared. The analysis on the comparisons of the change ratios of heat transfer coefficient due to these factors was conducted as well. The results are expected to be used for deeper research on the coupling mode of flowing liquid film heat transfer for further application.

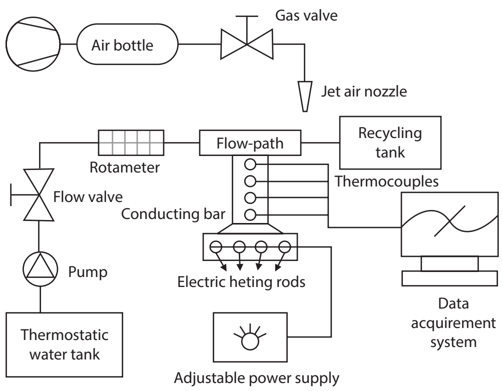

Figure 1. Schematic diagram of flowing liquid film with inserted metal foam porous layer subjected to air jet impingement

Experimental apparatus and process

Experimental apparatus

The experimental apparatus was comprised of a working fluid circulation system, an air supply system, an adjustable heating system, a test bench and a data acquirement system, as shown in fig. 1.

During operation, the deionized water served as working fluid was pumped to the liquid film flow-path in which the phase change took place within porous layer and on the outside surface of porous layer. The thermal insulation was set around the conducting bar and flow path, thus the less heat loss occurred from the envelop enclosure of flow path to the outside. Due to the liquid fluid with the inserted metal foam, the thickness of liquid fluid layer changed from $\delta_f = 0.0005$ m to $\delta_f = 0.002$ m, the flowing liquid layer is considered as a flowing liquid film. The flow rate of working fluid was controlled and measured through a regulating valve and a rotameter. Residual water at flow-path exit was recycled to a recycling tank. The generated vapor was dissipated by jet air and the phase change process continued. The surface of flow path tended to a smooth plate and the velocity of liquid fluid changed from $V_f = 0.018$ m/s to $V_f = 0.054$ m/s, thus the friction along flow path influenced less in tests.

The flow-path was made up of a specially manufactured metal square cavity ($0.14 \times 0.04 \times 0.015$ m), with the metal foam porous layer embedded on the top groove ($0.065 \times 0.023 \times 0.01$ m), as shown in figs. 2(a) and 2(c). The gap between the porous layer bottom and the heated wall surface was adjusted using shims at certain thicknesses. Once the distance was fixed, the shim was taken away and the metal foam was adhered to the surrounding wall to avoid the side flow and to control the thickness of liquid film when the liquid fluid passed through the flow path. As the insulation cotton was set around the flow path, less heat was transferred from the side passages of flow path to the outside.

Four testing points, each diameter in 0.001 m, depth in 0.01 m and separation distance in 0.01 m, were averagely located along the axial direction of the conducting bar that had a diameter of 0.02 m, as shown in fig. 2(b). These equidistantly distributed testing points were designated for inserting thermocouples to averagely calculate the heat flux from the heating base to the heated wall surface using Fourier's law. Both the conducting bar and the heated wall were made of copper. Four thermocouples were inserted in the outer surface of thermal insulation cotton around for heat loss calculation.

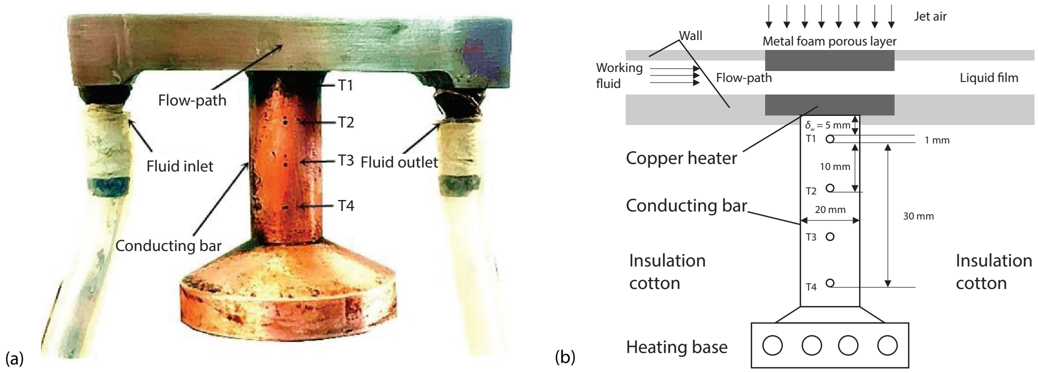

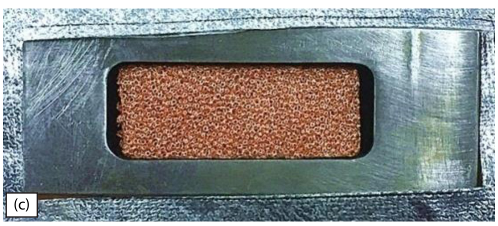

Figure 2. (a) Flow-path and conducting bar, (b) specifications of flow-path and conducting bar, (c) flow-path and metal foam porous layer enwrapped by insulation

Experimental preparation

All thermocouples were calibrated within minimized error. Based on the primary test of error, the uncertainty of the temperature measurement of thermocouples was less than 0.1 °C, while the minimum temperature difference of each adjoining thermocouples was 1.5 °C. Therefore, the uncertainty of the heat flux was less than 6.7%.

All thermal contact surfaces were adhered by highly conductive thermal grease (8.5 W/mK) to keep efficient heat transfer. The temperatures of jet air and the working fluid stored in the thermostatic tank were remained at 25 °C.

Experimental process

In each experiment, the electric heating power was increased from 0 to 250 W by controlling the voltage regulator, with a gradual growing interval of 20 W for every data collection. Once the values of each thermocouple varied within a range of 0.2 °C in 20 minutes, the heat transfer state was considered to be steady, then the values were recorded by the data acquirement system. When the heated wall temperature reached near 160 °C, the boiling phenomena tended to be intense and the experiment terminated manually. The variation curve of heat flux *vs.* time in the tests is plotted in fig. 3, and each entire experimental process lasted about 5 hours.

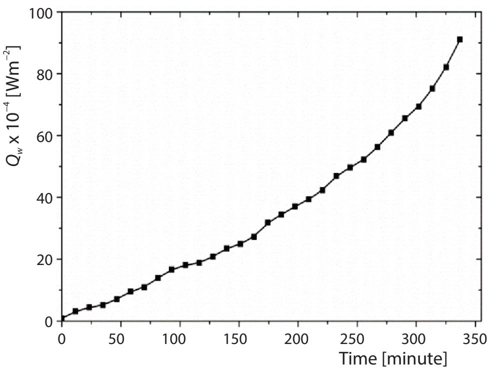

Figure 3. Change of heat flux *vs.* time in tests

The heat flux through the conducting bar Q_w, the heat loss through the thermal insulation material Q_{ins}, the heated wall temperature T_w and the corresponding local heat transfer coefficient h_w were calculated:

$$Q_w = -k_{cp} \frac{dT}{dy} \tag{1}$$

$$Q_{ins} = \frac{2 \cdot 0.05 \pi k_{ins} (T_{ave} - T_{ins})}{\ln \frac{160}{10}} \tag{2}$$

$$T_w = T_1 - \frac{(Q_w - Q_{ins}) \delta_w}{k_{cp}} \tag{3}$$

$$h_w = \frac{Q_w - Q_{ins}}{T_w - T_f} \tag{4}$$

where k_{cp} and k_{ins} are the thermal conductivities of copper and thermal insulation material, respectively, dT/dy – the temperature gradient along axial direction of the conducting bar, T_1 – the temperature of top thermocouple on the conducting bar, T_{ave} – the average temperature of the four thermocouples on the conducting bar, T_{ins} – the average temperature of the four thermocouples around the thermal insulation material, δ_w – the distance between the top thermocouple and the heated wall surface, and T_f – the liquid film inlet temperature.

Results and discussion

The experiment was conducted at standard atmospheric pressure, ambient temperature of 25 °C and relative humidity of 50-60%. In the study of an individual factor, the other factors remained constant.

Effect of liquid film velocity

Figure 4 demonstrates the evolution curves of heated wall temperature and the corresponding local heat transfer coefficient *vs*. heat flux for V_f = 0.018 m/s, 0.036 m/s, and 0.054 m/s, respectively, at constant conditions of: V_a = 4 m/s, δ_f = 0.002 m, ε = 0.9, and H_n = 0.1 m. As can be seen, the lower heated wall temperature and higher heat transfer coefficient can be obtained at the same heat flux for V_f = 0.054 m/s, so, the increase in liquid film velocity lowers the average heated wall temperature and enhances the heat transfer performance of heated wall along with the growing heat flux. This is because the increase in fluid speed near the heated wall surface leads to a thinner boundary-layer and a lower thermal resistance which favor the improvement of heat transfer in the phase change of liquid film.

The comparison of the curves in fig. 4(a) shows that both three temperature evolution curves appear steady change below 140 °C, whereas obvious fluctuations occur at a higher temperature. When the superheat of heated wall reaches a certain value, the heated wall temperature remains almost constant or grows slowly with the increasing heat flux, where the onset of boiling is identified and fluctuations initiate. According to the research of Narayanan *et al*. [13], based on different heat transfer regimes, the entire heat transfer process can be divided into three-stages: firstly at relatively low heat fluxes, the single phase convection occupies main position in total heat transfer, thus the heated wall temperature curve evolves linearly; secondly at higher heat fluxes but still not reaching to be boiling, the evaporation dominates the main proportion in total heat transfer instead of convection, the heated wall temperature appears a slight slowdown tendency in growth due to the latent heat of evaporation; finally at relatively high heat fluxes that the boiling initiates, the main form of heat transfer is changed to be boiling. In the case of boiling, the phase change keeps happening and the temperature fluctuation further intensifies due to the new heat balance which is ceaselessly established. The more amount of heat that dissipates rapidly due to phase change that leads to an instantaneously decrease in heated wall temperature, whereas the vapor or vapor bubble would not be able to escape from the vapor-liquid interface and heated wall surface in time due to the impinging of jet air, and it influences the heat dissipation the outside in the vapor-liquid phase change process. This hysteresis effect further interprets the fluctuation phenomenon.

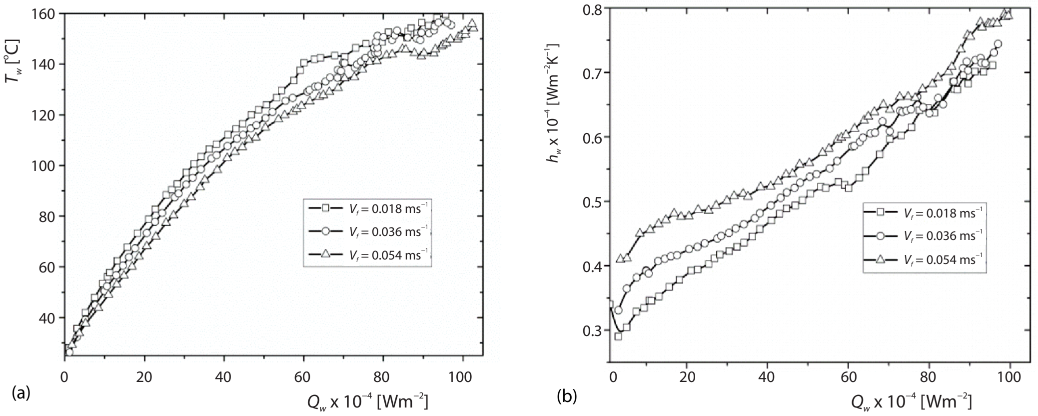

Figure 4. Flowing liquid film with inserted porous layer subjected to air jet impingement at V_f = 0.018 m/s, 0.036 m/s, and 0.054 m/s, respectively, for constant conditions of V_a = 4 m/s, δ_f = 0.002 m, ε = 0.9, and H_n = 0.1 m; (a) heated wall temperature *vs*. heat flux, (b) local heat transfer coefficient *vs*. heat flux

As can be seen in fig. 4(b), for some partial segments near 800 kW/m^2, the comparison of the heat transfer coefficients between $V_f = 0.018$ m/s and $V_f = 0.036$ m/s shows an interesting observation that the lower liquid film velocity even brings a greater heat transfer coefficient. The cause of this phenomenon is that at relatively high heat fluxes where boiling initiates, the boiling accounts for a more substantial proportion in total heat transfer at a slower fluid speed than that of at a higher fluid speed, since lower fluid speed causes more time to be used to heat a unit volume of fluid so that the phase change process is enhanced. Therefore, the heated wall temperature is declined at the lower flow velocity of liquid film and the heat transfer coefficient is enhanced by the more effective cooling effect due to phase change.

Effect of air jet velocity

Figure 5 shows the variation curves of heated wall temperature and the corresponding local heat transfer coefficient along with the growing heat flux for $V_a = 4$ m/s, 8 m/s. and 12 m/s, respectively, at constant conditions of: $V_f = 0.036$ m/s, $\delta_f = 0.002$ m, $\varepsilon = 0.9$, and $H_n = 0.1$ m. It is clear that at the same heat flux, the heated wall temperature declines as the air jet velocity increases. As the higher speed of jet air occurred, the disturbance of air-flow is promoted and the diffusion of vapor-air mixture is enhanced, as well as the vapor concentration gradient at the porous layer outlets is amplified. Also the larger impinging speed creates a thinner boundary-layer around the stagnation point of the porous layer, so, the thermal resistance drops consequently. Besides, according to the report of Yakkatelli *et al.* [21], due to the increase in air velocity, the transition from laminar flow to turbulent flow allows more air to enter the pores of porous layer as well as reduces the flow deflection, and the air-flow penetrates more deeply into the foam metal layer, as a result, the mass transfer is improved. Thus, lower heated wall temperature and higher local heat transfer coefficient occur at the same heat flux.

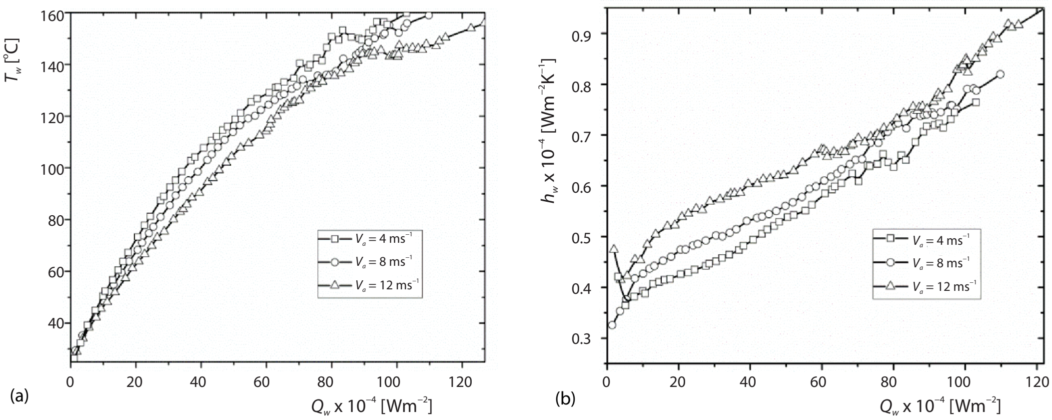

Figure 5. Flowing liquid film with inserted porous layer subjected to air jet impingement at $V_a = 4$ m/s, 8 m/s and 12 m/s, respectively for constant conditions of $V_f = 0.036$ m/s, $\delta_f = 0.002$ m, $\varepsilon = 0.9$, and $H_n = 0.1$ m; (a) heated wall temperature *vs.* heat flux, (b) local heat transfer coefficient *vs.* heat flux

Effect of liquid film thickness

The evolution curves of heated wall temperature and the corresponding local heat transfer coefficient for $\delta_f = 0.002$ m, 0.001 m, and 0.0005 m, respectively, are shown in fig. 6, at constant conditions of: $V_f = 0.036$ m/s, $V_a = 8$ m/s, $\varepsilon = 0.9$, and $H_n = 0.1$ m. In this experiment, the liquid film thickness is considered to be approximately equal to the distance between the heated wall surface and the porous layer bottom. In fact, according to the research of Narayanan *et al*. [13], at relatively low heat fluxes, the liquid-vapor interface locates closer to porous layer bottom. Along with the heat flux increases, the level of liquid-vapor interface ascends until it approaches near the porous layer upper outlets. Lower heated wall temperature and higher heat transfer coefficient occur for δ_f = 0.0005 m at the same heat flux, thus, the heat transfer is enhanced due to the decrease in liquid film thickness. The comparison of curves of δ_f = 0.001 m and δ_f = 0.002 m shows a limited decrease in the heated wall temperature at the same heat flux, with a tiny promotion of the heat transfer coefficient obtained. While the comparison of curves of δ_f = 0.0005 m and δ_f= 0.001 m presents a remarkable drop on heated wall temperature and a significant increase in heat transfer coefficient. Owing to the heat transfer characteristics of coupling of flowing liquid film and porous layer, the thinner liquid film reduces the thermal resistance of both conduction and convection. Meanwhile, it also leads to a smaller distance between the actual liquid-vapor interface and the porous layer outlets. Additionally, due to the decrease of the gap between the heated wall and the metal foam bottom, the more volume occupied by the porous layer pushed more fluid into the liquid film zone, which results in a higher speed of fluid near the heated wall. Thus, the micro-convection inside the porous layer, the diffusion of vapor-air mixture and the heat transfer near the heated wall surface can be all enhanced.

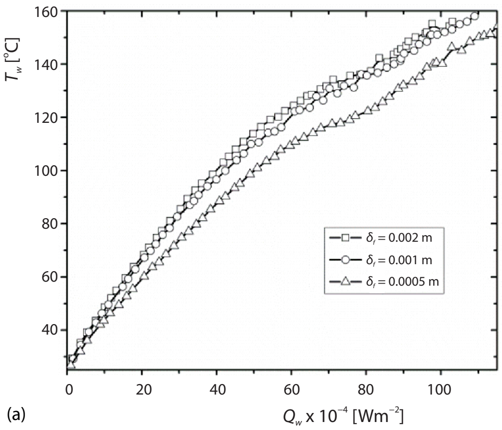

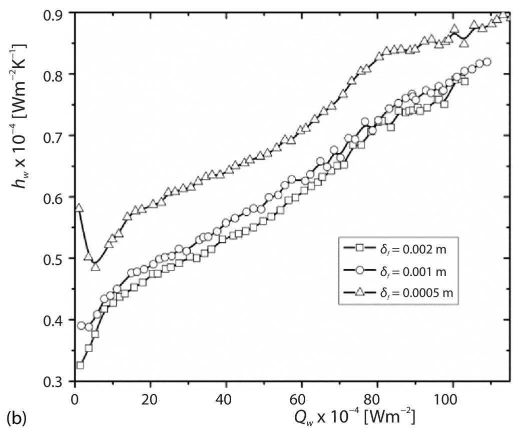

Figure 6. Flowing liquid film with inserted porous layer subjected to air jet impingement at δ_f = 0.002 m, 0.001 m, and 0.0005 m, respectively, for constant conditions of V_f= 0.036 m/s, V_a = 8 m/s, ε = 0.9, and H_n = 0.1 m; (a) heated wall temperature *vs.* heat flux, (b) local heat transfer coefficient *vs.* heat flux

Effect of porosity

Figure 7 illustrates the evolution curves of heated wall temperature and the corresponding local heat transfer coefficient for ε = 0.9, 0.96, and 1 with corresponding Φ = 15 PPI, 30 PPI, and 0, respectively, at constant conditions of: V_f = 0.036 m/s, V_a = 8 m/s, δ_f = 0.0005 m, and H_n = 0.1 m. The result of ε = 1 stands for the case of bare flowing liquid film without inserting any porous layer. At the heat flux less than 600 kW/m^2, the heat transfer characteristics of ε = 0.9 and ε = 0.96 are similar, but all slightly greater than that of the no porous layer situation. While the heat flux is larger than 600 kW/m^2, similar trends are exhibited between the heat transfer characteristics of ε = 0.96 and the no porous layer situation, but the lower heated wall temperature and higher heat transfer coefficient are obtained at ε = 0.9 than the former two, thus, the heat transfer is enhanced. Based on the property of porous material, both the heat conductivity and convection are ameliorated through the porous medium matrix. The higher thermal conductivity and specific area can be obtained in the $\varepsilon = 0.9$ porous layer than that of $\varepsilon = 0.96$ porous media, which serves as the dominant function on the heat transfer at the heat flux above 600 kW/m^2 in the tests. The increase in the porosity from $\varepsilon = 0.9$ to $\varepsilon = 0.96$ leads to more convection in the porous layer, as results, the heat transfer coefficients in the $\varepsilon = 0.96$ porous media are slightly higher than that of the $\varepsilon = 0.9$ porous media at the heat flux below 600 kW/m^2.

For the pore size in a porous layer with certain porosity, the larger specific area and more capillary force can be obtained in the porous layer with smaller pore size, which favors the heat transfer. The liquid level rises and liquid phase occupies more volume inside the porous layer with smaller pore size due to relatively larger capillary force so that the heat transfer area between the liquid and the solid matrix is increased. However, the convection drops in the porous layer with a decrease in pore size, and it is disadvantage to the heat transfer. At the heat flux below a certain value, more heat transfer contribution of sensible cooling than that of phase change occurs. The vapor and vapor bubble escape from smaller pore more difficulty when more phase change happens at the relatively higher heat fluxes, and it influences the heat transfer of phase change greatly. Thus, the domain effects of pore size in a porous layer on the heat transfer needs to be investigated, which are connected with the heat flux.

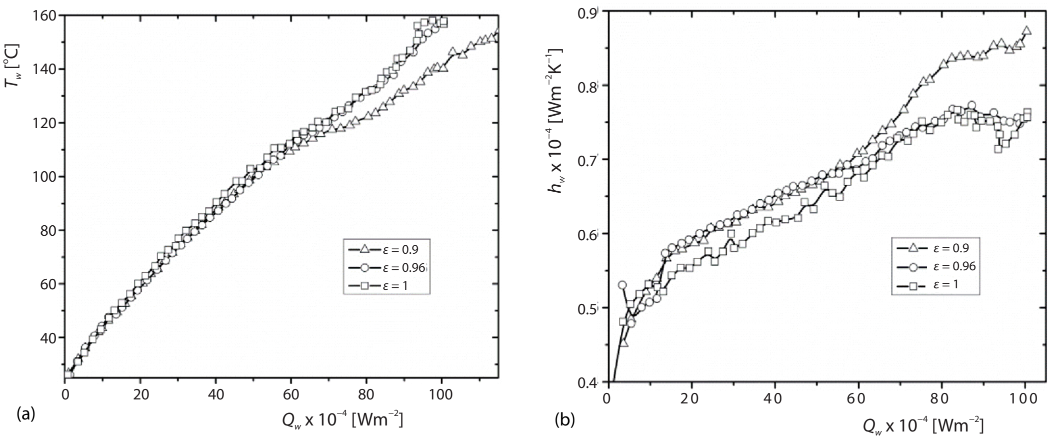

Figure 7. Flowing liquid film with inserted porous layer subjected to air jet impingement at $\varepsilon = 0.9$, 0.96, and 1 with corresponding Φ = 15 PPI, 30 PPI, and 0, respectively, for constant conditions of $V_f = 0.036$ m/s, $V_a = 8$ m/s, $\delta_f = 0.0005$ m, and $H_n = 0.1$ m; (a) heated wall temperature *vs.* heat flux, (b) local heat transfer coefficient *vs.* heat flux

Comparisons of change ratios of heat transfer coefficient

Figure 8 shows the evolution curves of change ratios of heat transfer coefficient owing to the variations of liquid film velocity, air jet velocity, liquid film thickness and porous layer porosity, compared with the heat transfer coefficient at $V_f = 0.018$ m/s, $V_a = 4$mm/s, $\delta_f = 0.002$ m, and $\varepsilon = 1$, respectively.

Figure 8(a) illustrates the change ratios of heat transfer coefficient at $V_f = 0.054$ m/s and $V_f = 0.036$ m/s, respectively, compared with that of $V_f = 0.018$ m/s. At heat flux of 100 kW/m^2, as the V_f experiences a three-fold increase from 0.018-0.054 m/s, the change ratio of heat transfer coefficient reaches 35% as the first peak value; then as the heat flux grows, the change ratio witnesses a deterioration until it reaches only 10%; afterwards, it shows a slight rise to the second peak value of 17% at heat flux of 600 kW/m^2, and then rapidly slips below 10%. Similar tendency is expressed on the curve of V_f= 0.036 m/s. The comparison reveals that the improvement effect according to the increase in liquid film velocity mainly acts on the heat transfer of relatively low heat fluxes.

Figure 8(b) presents the change ratios of heat transfer coefficient at V_a = 12 m/s and V_a = 8 m/s compared with the case of V_a = 4 m/s. For a two-fold increase of V_a from 4-8 m/s, the change ratio of heat transfer coefficient fluctuates below 12%, and the two peak values reach up to 11% and 9% at 300 kW/m^2 and 800 kW/m^2, respectively. The change ratio as a result of a three-fold increase of V_a from 4-12 m/s achieves two peak values of 27% and 15%, respectively, and the significant heat transfer improvement occurs at relatively low heat fluxes instead of high heat fluxes. Due to the increase in air jet speed, the mass transfer is enhanced, but the decline of liquid-vapor interface temperature and pressure may act as an obstacle to the further evaporation and boiling.

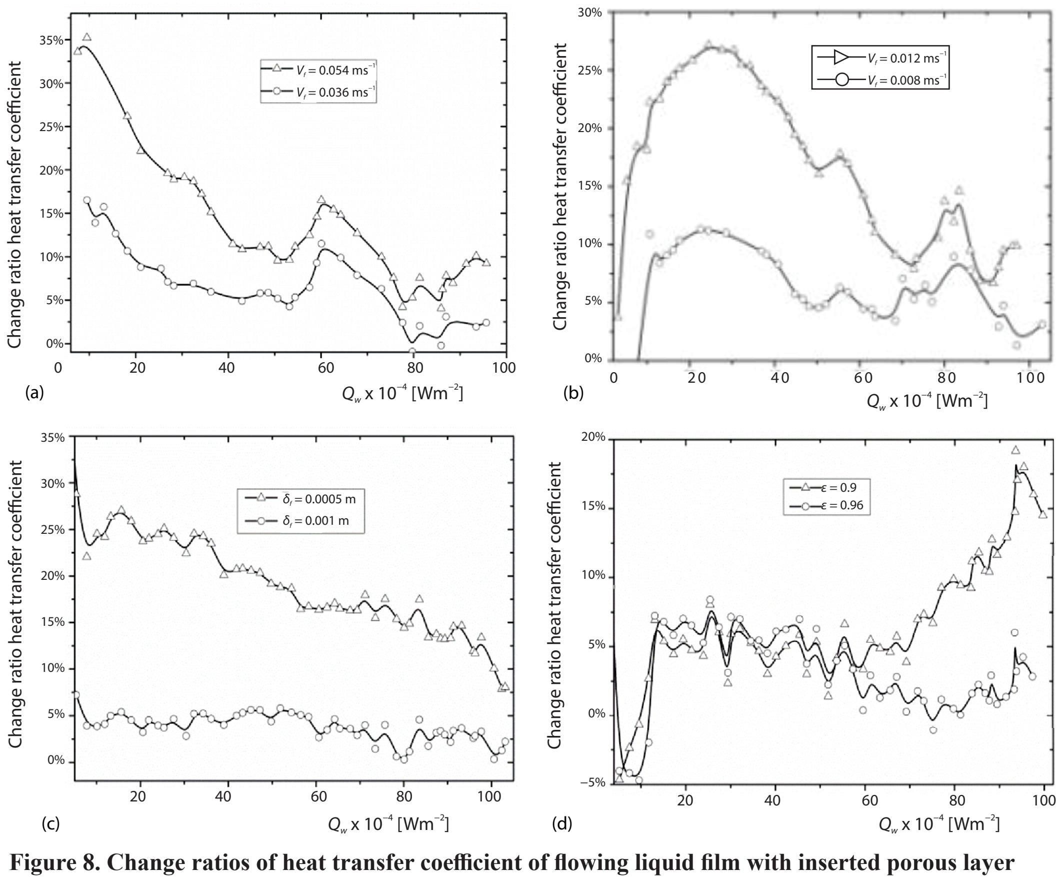

Figure 8. Change ratios of heat transfer coefficient of flowing liquid film with inserted porous layer subjected to air jet impingement, due to the effect of; (a) liquid film velocity, (b) air jet velocity, (c) liquid film thickness, (d) porous layer porosity, compared with the heat transfer coefficients at V_f = 0.018 m/s, V_a = 4 m/s, δ_f = 0.002 m, and ε = 1, respectively

Figure 8(c) contains the change ratios of heat transfer coefficient at δ_f = 0.0005 m and δ_f = 0.001 m compared with that of δ_f = 0.002 m. In the case of reducing δ_f from 0.002-0.001 m, the change ratio of heat transfer coefficient fluctuates around 5% showing a limited improvement. When further reducing δ_f from 0.002 m to a quarter (δ_f = 0.0005 m), the change ratio is substantially increased, with the highest value of 27% at heat flux of 180 kW/m^2. Along with the growing heat flux, it constantly deteriorates with the minimum value of 10% occurring in the end. So, minimizing the liquid film thickness might be the productive approach for heat transfer promotion, and the improvement effect is considerable in both cases of low and high heat fluxes.

Figure 8(d) shows the change ratios of heat transfer coefficient at $\varepsilon = 0.9$ and $\varepsilon = 0.96$ compared with that of no porous layer situation ($\varepsilon = 1$). For $\varepsilon = 0.96$, the improvement mainly focuses on the relatively low heat flux stage, with the peak value of change ratio reaching 8% at 250 kW/m^2; then as heat flux exceeds 600 kW/m^2, the change ratio fluctuates basically below 5%. In the situation of $\varepsilon = 0.9$, the change ratio appears a slight wave below 10% at the heat flux less than 600 kW/m^2, but then is greatly enhanced until the peak value of 19% at 950 kW/m^2. Based on the phenomenon, to some extent the lower porosity brings greater heat transfer coefficient, but the improvement effect on heat transfer mainly plays a role in the case of high heat fluxes.

Conclusions

The experiment of heat transfer of flowing liquid film with inserted metal foam porous layer subjected to air jet impingement has been conducted. The factors of liquid film velocity, air jet velocity, liquid film thickness and material porosity have impact on heat transfer performance of flowing liquid film to different degrees at various heat fluxes. The comparisons of the change ratios of heat transfer coefficient due to those factors reveal the mechanism of heat transfer in the process of flowing liquid film coupling with jet air and porous layer.

The summary of the major results can be concluded.

- The increase in liquid film velocity enhances the cooling performance, and for a three-fold increase from 0.018-0.054 m/s, the change ratio nearly reaches up to 35% and 15%, respectively at relatively low and high heat fluxes, thus the improvement effect of liquid film velocity on heat transfer coefficient is focused on the stage of relatively low heat fluxes.
- The increase in air jet velocity can improve the heat transfer performance, and at relatively low heat fluxes, the maximum change ratio according to a two-fold increase of air jet velocity is only 12% whilst for a three-fold air speed increase it can be up to 27%; at relatively high heat fluxes, both the change ratios due to the two-fold and three-fold increase of air jet velocity are not significant. Thus, the increase in air jet velocity mainly improves the heat transfer coefficient in the case of relatively low heat fluxes, and the enhancement at relatively high heat fluxes situation is restricted.
- The decrease in liquid film thickness increases the heat transfer coefficient, and further reducing the thickness up to a quarter of the original value leads to a more substantial growth in heat transfer coefficient, and the change ratio can be up to 10-27%. The improvement effect of minimizing the liquid film thickness on heat transfer coefficient can act on both occasions of low and high heat fluxes.
- Compared with bare flowing liquid film, inserting porous layer can improve the heat transfer performance of flowing liquid film. The decrease of porosity from 0.96-0.9 leads to a increase in the heat transfer coefficient when the heat fluxes are above a certain value, and the change ratio of heat transfer coefficient for porosity of 0.9 can amount up to 19% while that for porosity of 0.96 only remains below 5%. The variations of thermal conductivity, specific area and convection in the porous layer are related to its porosity, which influence the heat transfer coefficients more greatly with the increase in the heat flux.

- Based on the previous results, by strengthening the control on these factors, the approach on deeper optimization of the heat transfer performance in the applications of cooling system promotion is available.

Acknowledgment

The current work is financially supported by the National Natural Science Foundation of China (No. 51276107), the Innovation Program of Shanghai Municipal Education Commission (14ZZ142) and the Ministry of Transport Application Foundation Project (2013319810150).

Nomenclature

D – diameter, [m]
H_n – nozzle height, [m]
h_w – local heat transfer coefficient of heated wall, [Wm^{-2}K^{-1}]
k_{cp} – thermal conductivity of copper, [Wm^{-1}K^{-1}]
k_{ins} – thermal conductivity of insulation material, [Wm^{-1}K^{-1}]
Q_{ins} – heat loss through thermal insulation material, [Wm^{-2}]
Q_w – heat flux through the heated wall, [Wm^{-2}]
T_w – temperature of heated wall, [K°C^{-1}]
T_f – temperature of liquid film, [K°C^{-1}]
V_a – air jet velocity, [ms^{-1}]
V_f – liquid film velocity, [ms^{-1}]
y – axial direction

Greek symbols

δ_f – thickness of liquid film, [m]
δ_w – distance between the top thermocouple and heated wall surface, [m]
ε – porosity of metal foam
Φ – pore density, [PPI]

Subscripts

a – air
cp – copper
f – liquid film
ins – insulation material
m – metal foam
n – nozzle
w – heated wall

References

[1] Wang, H., *et al.*, An analytical Solution for the Total Heat Transfer in the Thin-Film Region of an Evaporating Meniscus, *International Journal of Heat and Mass Transfer*, *51* (2008), 25-26, pp. 6317-6322

[2] Souza A G U D, Jr. J. R. B., Spray Cooling of Plain and Copper-Foam Enhanced Surfaces, *Experimental Thermal and Fluid Science*, *39* (2012), May, pp. 198-206

[3] Crepinsek, M., Park, C., Experimental Analysis of Pump-Assisted and Capillary-Driven Dual-Evaporators Two-Phase Cooling Loop, *Applied Thermal Engineering*, *38* (2012), 1, pp. 133-142

[4] Zhou, Y. Y., Yu, J. L., *et al.*, A Study on Flow and Heat Transfer Characteristics for Saturated Falling-Film Evaporation of Liquid Oxygen in a Vertical Channel, *International Journal of Heat and Mass Transfer, 55* (2012), 23-24, pp. 7218-7222

[5] Qu, W., *et al.*, Effects of Radius and Heat Transfer on the Profile of Evaporating Thin Liquid Film and Meniscus in Capillary Tubes, *International Journal of Heat and Mass Transfer*, *45* (2002), 9, pp.1879-1887

[6] Shirazy, M.bR.bS.,Frechette, L. G., Capillary and Wetting Properties of Copper Metal Foams in the Presence of Evaporation and Sintered Walls, *International Journal of Heat and Mass Transfer*, *58* (2013), 1-2, pp. 282-291

[7] Lee, S., Koroglu, B., *et al.*, Experimental Investigation of Capillary Assisted Solution Wetting and Heat Transfer Using a Micro-Scale, Porous-Layer Coating on Horizontal-Tube, Falling-Film Heat Exchanger, *International Journal of Refrigeration*, *35* (2012), 4, pp. 1176-1187

[8] Sosnowski, P., *et al.*, Numerical Model for Thin Liquid Film with Evaporation and Condensation on Solid Surfaces in Systems with Conjugated Heat Transfer, *International Journal of Heat and Mass Transfer*, *66* (2013), Nov., pp. 382-395

[9] Shahzad, M. W., Myat, A., *et al.*, Bubble-Assisted Film Evaporation Correlation for Saline Water at Sub-Atmospheric Pressures in Horizontal-Tube Evaporator, *Applied Thermal Engineering*, *50* (2013), 1, pp. 670-676

[10] Nasr, A., Al-Ghamdi, A. S., Numerical Study of Evaporation of Falling Liquid Film on one of Two Vertical Plates Covered with a Thin Porous Layer by Free Convection, I*nternational Journal of Thermal Sciences*, *112* (2017), Feb., pp. 335-344

[11] Terzi, A., Foudhil, W. S., *et al*., Liquid Film Evaporation Inside an Inclined Channel: Effect of the Presence of a Porous Layer, *International Journal of Thermal Sciences*, *109* (2016), Nov., pp. 136-147
[12] Leu, J. S., *et al*., Heat and Mass Transfer for Liquid Film Evaporation Along a Vertical Plate Covered with a Thin Porous Layer, *International Journal of Heat and Mass Transfer*, *49* (2006), 11-12, pp. 1937-1945
[13] Narayanan, S., *et al*., Heat and Mass Transfer during Evaporation of Thin Liquid Films Confined by Nanoporous Membranes Subjected to Air Jet Impingement, *International Journal of Heat and Mass Transfer*, *58* (2013), 1-2, pp. 300-311
[14] Narayanan, S., *et al*., On-Chip Thermal Management of Hotspots Using a Perspiration Nanopatch, *Journal of Micromechanics and Microengineering*, *20* (2010), 7, 075010
[15] Zhao, T. S., Coupled Heat and Mass Transfer of a Stagnation Point Flow in a Heated Porous Bed with Liquid Film Evaporation, *International Journal of Heat and Mass Transfer*, *42* (1999), 5, pp. 861-872
[16] Wong, K. C., Indran, S., Impingement Heat Transfer of a Plate Fin Heat Sink with Fillet Profile, *International Journal of Heat and Mass Transfer*, *65* (2013), Oct., pp. 1-9
[17] Wong, K. C., Saeid, N. H., Numerical Study of Mixed Convection on Jet Impingement Cooling in a Horizontal Porous Layer-Using Brinkman-Extended Darcy model, *International Journal of Thermal Sciences*, *48* (2009), 1, pp. 96-104
[18] Wong, K. C., Saeid, N. H., Numerical Study of Mixed Convection on Jet Impingement Cooling in an Open Cavity Filled with Porous Medium, *International Communications in Heat and Mass Transfer*, *36* (2009), 2, pp. 155-160
[19] Wong, K. C., Thermal Analysis of a Metal Foam Subject to Jet Impingement, *International Communications in Heat and Mass Transfer*, *39* (2012), 7, pp. 960-965
[20] Dorea, F. T., De Lemos, M. J. S., Simulation of Laminar Impinging Jet on a Porous Medium with a Thermal Non-Equilibrium Model, *International Journal of Heat and Mass Transfer*, *53* (2010), 23-24, pp. 5089-5101
[21] Yakkatelli, R., *et al*., A Visualization Study of the Flow Dynamics of a Single Round Jet Impinging on Porous Media, *Experimental Thermal and Fluid Science*, *34* (2010), 8, pp. 1008-1015

Paper submitted: October 14, 2017
Paper revised: January 13, 2018
Paper accepted: February 6, 2018